Flight-Test Evaluation of Airframe Noise Mitigation Technologies

Mehdi R. Khorrami,[1] David P. Lockard,[2] William M. Humphreys, Jr.[3]
NASA Langley Research Center, Hampton, VA, 23681, USA

and
Patricio A. Ravetta[4]
AVEC Inc., Blacksburg, Virginia 24060, USA

A series of flight tests targeting airframe noise reduction was planned and executed under the NASA Flight Demonstrations and Capabilities project. The objectives of the tests were two-fold: to evaluate the aeroacoustic performance of several noise reduction technologies in a relevant environment and to generate a comprehensive database for advancing the state of the art in simulation-based airframe noise prediction methodologies. These technologies – an Adaptive Compliant Trailing Edge flap, main landing gear fairings, and gear cavity treatments – were integrated on a NASA Gulfstream G-III aircraft to determine their effectiveness, both on a component-level (individually) and a system-level (combined) basis. With the aircraft flying an approach pattern and the engines set at ground idle, extensive acoustic measurements were acquired using a phased microphone array system. Detailed analyses of the gathered acoustic data clearly demonstrate that significant noise reduction was achieved for the flap and main landing gear components.

Nomenclature

AOA = Angle of attack
C_P = Pressure coefficient
f = Frequency
M = Mach number
V = Velocity

Acronyms

ACTE = Adaptive Compliant Trailing Edge
AFB = Air Force Base
AFRC = Armstrong Flight Research Center
AFRL = U. S. Air Force Research Laboratory
ARMD = Aeronautics Research Mission Directorate
EPNL = Effective perceived noise level
ERA = Environmentally Responsible Aviation
FAA = Federal Aviation Administration
FDC = Flight Demonstrations and Capabilities
IAS = Indicated air speed
IASP = Integrated Aviation Systems Program
LaRC = Langley Research Center
MLG = Main landing gear
NR = Noise reduction
PKF = Porous knee fairing

---

[1] Aerospace Engineer, Computational AeroSciences Branch, Associate Fellow AIAA.
[2] Aerospace Engineer, Computational AeroSciences Branch, Senior Member AIAA.
[3] Aerospace Engineer, Advanced Measurements and Data Systems Branch, Associate Fellow AIAA.
[4] Co-owner, Chief Research Engineer, Senior Member AIAA.

PSD = Power spectral density
SCRAT = SubsoniC Research Aircraft Testbed
SNR = Sound to Noise ratio
SoDAR = Sound Detection and Ranging
SPL = Sound pressure level
TAS = True air speed
UF = Upper fairings

I. Introduction

The NASA Aeronautics Research Mission Directorate (ARMD) maintains a sustained effort toward reducing the impact of civil aviation operations on community noise. The introduction of aircraft with smaller noise footprints is viewed as a key enabler of the anticipated growth in air travel [1, 2]. To achieve a substantial reduction in aircraft noise, equal attention must be paid to the propulsion and airframe components of noise. Airframe noise is the principal component during aircraft landing, when the undercarriage and wing high-lift devices, such as flaps and slats, are deployed [3]. The ARMD is pursuing the development and maturation of viable technologies that provide significant airframe noise mitigation without negatively affecting aircraft aerodynamic performance.

Effective airframe noise reduction (NR) concepts can be developed through persistent, systematic considerations of their aeroacoustic performance via model-scale ground tests and high-fidelity simulations [4–7]. Ultimately, however, the achievable system-level performance of the NR technologies must be evaluated in flight, whereby important questions such as scale, installation, and integration effects can be determined and addressed in a relevant environment [8–10]. Under the Flight Demonstrations and Capabilities (FDC) project of the NASA Integrated Aviation Systems Program, researchers are evaluating the aeroacoustic performance of several NR technologies while advancing the state of the art in simulation-based airframe noise prediction methodologies. The technologies being evaluated include the Adaptive Compliant Trailing Edge (ACTE) flap, main landing gear fairings, and gear cavity treatments, all developed under the Environmentally Responsible Aviation (ERA) project.

To accomplish this task, a comprehensive flight test campaign comprised of several phases was planned and executed. During the first test, conducted in August–October of 2016, the ACTE flap was evaluated using two NASA Gulfstream G-III aircraft as testbeds. Extensive acoustic measurements were acquired using a NASA-developed phased microphone array system [11]. The airframe noise reduction levels achieved with this technology were measured, both on a component-level (landing gear retracted) and in the presence of the landing gear, relative to the unmodified "baseline" G-III configuration with the original Fowler flap system. The measured data indicated that the ACTE technology is highly effective, virtually eliminating flap noise. The second flight test, conducted during August–October of 2017, focused on assessing the effectiveness of the main landing gear fairings and the two gear cavity treatments. To determine the full extent of the noise reduction benefits, the main landing gear NR technologies were tested in combination with the ACTE flap. The elimination of flap noise through the use of the ACTE allowed us to determine the full extent of the noise reduction benefits achieved with the main landing gear treatments. The third flight test, conducted during March–May of 2018, evaluated the performance of the main gear fairings and the cavity treatments on the baseline G-III aircraft. Altogether, 47 flights encompassing nearly 1,100 passes over the microphone array were conducted during the three test campaigns.

Detailed analyses of the comprehensive aeroacoustic data gathered during the first and second flight tests are presented in this paper. Results from the first test indicate that the ACTE flap is highly effective, as application of the technology virtually eliminated aircraft flap noise. The analyses also show how well the landing gear concepts perform in substantially reducing noise from the main gear and the wheel cavity.

II. Test Aircraft and Test Site

All flight operations were conducted with two Gulfstream G-III aircraft based at the NASA Armstrong Flight Research Center (AFRC). The primary G-III used during the first and second tests was the SubsoniC Research Aircraft Testbed (SCRAT), also known by its tail number as "804" (see Fig. 1a) [12]. The 804 is a heavily instrumented testbed that allows many of the aircraft critical parameters, including its global position, angle of attack (AOA), and true airspeed (TAS) to be recorded during flight. For the tests, the original Fowler flaps were replaced with a set of ACTE flaps. The port wing of the aircraft is equipped with three streamwise rows of steady pressure ports along the span.

The second G-III aircraft (called by its tail number "808") used to acquire acoustic data was flown in its original Fowler flap configuration (see Fig. 1b) [12]. Except for a NovAtel GPS receiver, the 808 had no other research instrumentation onboard to provide key aircraft parameters such as AOA and TAS. Thus, the acoustic data acquired for 808 were only used to provide a first look at the noise levels associated with the baseline G-III configuration. The

data obtained for 808 were complemented with additional acoustic measurements of 804 obtained during the Spring 2018 test, when the latter aircraft was converted from the ACTE configuration back to its Fowler flap baseline. Both aircraft are equipped with original low-bypass ratio engines with newly installed hush kits. Detailed information for the 804 and 808 aircraft is provided in Ref. [12].

Both the 2016 and 2017 flight tests were conducted on the Rogers dry lake at Edwards Air Force Base (AFB) in southern California. The microphone array was deployed at the North end of runway 18L. The chosen location provided ample flat land for the disposition of various elements of the ground operations and data collection hardware.

a) NASA 804 (SCRAT) **b) NASA 808**

Fig. 1 Gulfstream G-III aircraft with ACTE flaps (left image) and Fowler flaps (right image).

A. Noise Reduction Technologies

With the ultimate goal of advancing the needed technologies for integrated wing designs with seamless, morphing control surfaces, the ACTE flap was developed under a joint effort among the U. S. Air Force Research Laboratory (AFRL), FlexSys, Inc., and the NASA ERA project. As described in Refs. [13–15], the ACTE flap replaces the conventional 19-foot-long aluminum Fowler flaps of the G-III with advanced, shape-changing flaps that form continuous bendable surfaces. At the inboard and outboard ends of the flap, 2 ft. wide transition sections produce continuous mating of the flap to the adjacent main wing segments, thus eliminating the side-edges found on a typical Fowler flap configuration. Figure 2 displays a picture of the ACTE concept applied to the 804 aircraft. Initial flight testing of the ACTE technology focused on the structural and aerodynamic aspects of the concept [13-15]; determination of its acoustic performance was left for subsequent tests.

The main landing gear (MLG) fairings, which were originally developed for testing on the larger Gulfstream G-V aircraft [7], had to undergo significant design alterations to fit into the slightly (10% – 15%) smaller G-III main landing gear [12]. Because of the relative size of the aircraft, no frequency scaling was necessary. During the refitting process, after each iteration cycle, the aeroacoustic performance of the redesigned fairings was evaluated, via simulations of the full-scale landing gear installed on a semi-span model of the G-III aircraft, to ensure that the noise reduction effectiveness of the fairings was maintained. Three to four cycles were required to achieve the appropriate outer mold line that would yield the expected aeroacoustic performance. This integrated use of the high-fidelity simulations was key to arriving at an optimal configuration while at the same time meeting a host of other operational requirements. The redesign and tailoring of the two gear cavity concepts from a G-V to a G-III aircraft was achieved without encountering any major difficulties.

A side-by-side comparison of the G-III MLG with and without the fairings is shown in Fig. 3. The fairings comprise the porous knee fairing (PKF) covering the front post plus an assortment of smaller fairings that are collectively referred to as upper fairings (UF). The porous knee fairing consists of two segments. The lower segment extends from the juncture of the torque tubes to the bottom of the lower shock tube and is form-fitted to allow clearance between the fairing and the wheels. The upper segment of the porous fairing is wider, and like the lower fairing, is restricted from extending too far aft to allow proper wheel clearance. To maintain the desired open-area-ratio, a total of 11,332 0.080 in. (2 mm) diameter holes extending through the body were drilled on the two PKF segments. The UF is composed of three smaller fairings. The inboard close-out fairing, which resides above the PKF and is form-fitted around the underlying components, includes a retract strut cap fairing where the side strut attaches to the upper torque tube. The inboard close-out fairing is not porous. The UF also includes an aerodynamically-shaped (teardrop) door strut fairing.

The two cavity treatments consist of the full-scale version of the stretchable mesh concept reported in Ref. [5] and a concept that combines chevrons at the leading edge with an acoustic foam treatment on the downstream side of the cavity. A close-up view of the two concepts, as installed on the 804 aircraft, is shown in Fig. 4.

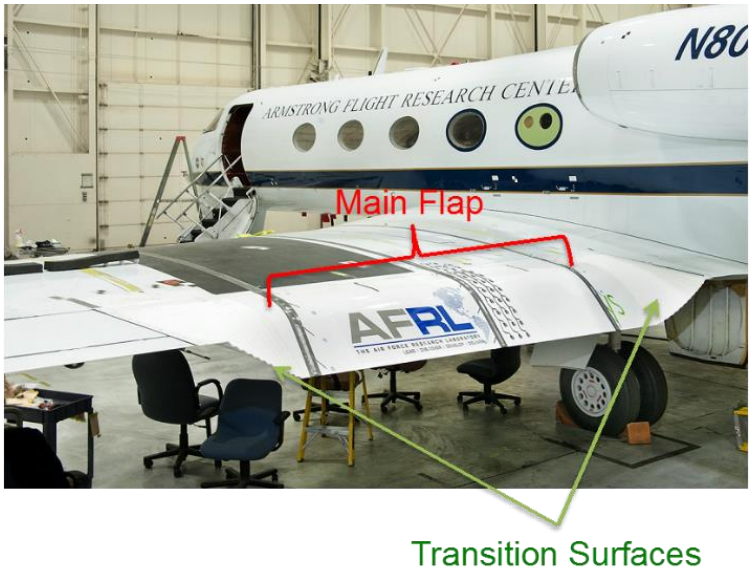

Fig. 2 NASA 804 (SCRAT) G-III aircraft with ACTE flaps.

a) Baseline **b) With fairings installed**

Fig. 3 Gulfstream G-III main landing gear. Baseline gear is shown in its compressed, on the ground state; the faired gear is depicted in its stretched, in-flight state.

a) Stretchable mesh **b) Chevrons and acoustic foam**

Fig. 4 Flight tested main gear cavity treatments as installed on 804 aircraft.

III. Test Procedure and Measurements

A short overview of the overall test procedure and supporting measurements is provided in this section. A full account of the flight and ground operations in support of the airframe noise test campaign is provided in Ref. [12].

A. Flight Pattern and Conditions

The tests were performed by flying the aircraft in a "racetrack" pattern, closely resembling the approach path for a typical landing as the airplane passed over the microphone array. A typical pass was usually completed within 4.5 to 5.5 minutes. During this period, the acquired array data was processed in near real-time for a few select frequencies on a relatively coarse grid. This "quick-look" capability was instrumental in assessing the quality of the measured data before completing the next pass. All passes were executed with the aircraft engines operating at "ground-idle" to minimize contamination of the acoustic measurements by propulsion noise. To the best of our knowledge, most previous airframe noise flight tests have been conducted with the engines set at "flight-idle," which corresponds to a thrust level that is 10% to 15% higher than ground-idle thrust. Given the low-bypass engines that power the G-III testbeds, we cannot emphasize enough how detrimental this higher thrust would have been to our measurements had we chosen to conduct the tests with engines at flight-idle settings.

During the flyover operations, the target altitude as the aircraft passed over the array center was 350 ft (106.7 m), with allowed deviations of ±50 ft (15.2 m) vertically. With respect to the center of the array, the allowable lateral deviation was ±35 ft (10.7 m). The airspeed tolerance was set at ±5 knots of the indicated airspeed (IAS). To determine velocity scaling, acoustic measurements for most configurations of interest were obtained at 140, 150, and 165 kts with the middle value representing the speed at which the majority of the measurements were taken. To ensure that the gathered data were statistically meaningful, multiple passes during each flight and multiple flights on different days were executed for most aircraft configurations. For these tests, and for a few select configurations, data collection spanned multiple years. As a result, pass-to-pass, day-to-day, and year-to-year variations in the measured noise signature and the resulting uncertainties can be evaluated and assessed. Acquisition of data over a sufficient number of passes on different days is essential to allow the variation of environmental conditions to be addressed.

B. Recording of Local Climate

Local weather conditions at Edwards AFB experience significant seasonal variation. Based on historical records, the August–October and February–April periods were selected as the best possible windows to maximize the number of acceptable test days. To obtain good-quality acoustic measurements, efforts were made to adhere to temperature, relative humidity, and wind restrictions specified by the Federal Aviation Administration (FAA) for noise certification purposes [16]. A window defined by the appropriate temperature-humidity combinations is depicted in Fig.5 by the green line. The corresponding gust/wind restrictions are listed in Table 1. Given the proximity of the test site to the Mojave Desert, operations during the most favorable weather conditions were difficult to maintain for a succession of flights. As a result, testing was also conducted on days when the temperature-humidity combinations were less than ideal. In this regard, those days when the local conditions were within the green-line region of Fig. 5 were dubbed as "good", those with conditions slightly outside the bottom line as "marginal", and those that were far from the line as "bad". Adherence to the wind restrictions was critical because of severely detrimental effects on mid- to high-

frequency noise by the wind and the lack of viable post-measurement corrections that could be applied to the acquired data [17]. Nevertheless, conducting flights on "marginal" or even "bad" days served two important purposes. First, the number of flight days was increased, thus expanding the statistical quality of the measured data. Second, the applicability and validity of various FAA-sanctioned weather corrections as applied to acoustic data acquired under less than ideal conditions could be studied closely. As demonstrated in Ref. [17], the corrections for atmospheric absorption became questionable only for extremely "bad" days.

Most flight operations were conducted early in the morning, around sunrise, when atmospheric turbulence was generally low and thermal effects (temperature inversions) ranged from mild to moderate (15º F or 8.3° C over 400 ft (122 m)). The meteorological conditions at the test site were recorded every hour with a tethered aerostat and every minute with two ground stations, one installed on top of the array data van at a height of 30 ft (10 m) and the other installed upstream of the array at a height of 10 ft (3 m). The aerostat-mounted sensors recorded temperature, pressure, relative humidity, and wind profiles as they were raised to an altitude of 550 ft (168 m). Unfortunately, during the 2016 test campaign some of the sensors on the balloon did not function properly. To remedy this shortcoming, the balloon-mounted sensors were replaced with more robust models for the 2017 test campaign. In addition, vertical profiles of wind speed and direction were obtained from a SoDAR (Sound Detection And Ranging) instrument deployed in the vicinity of the balloon launch area.

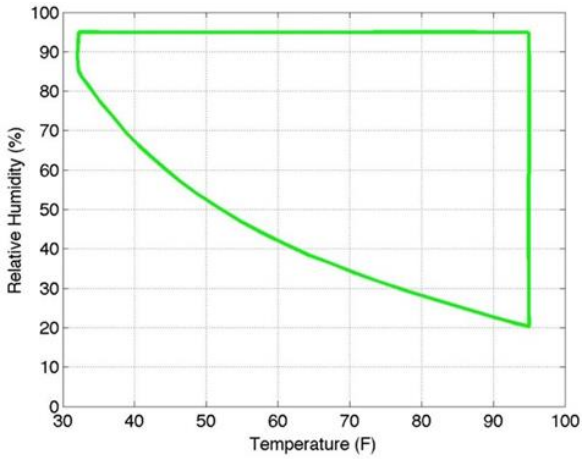

Fig. 5 Temperature and relative-humidity combinations favorable to acoustic measurements.

Table 1 Wind restrictions.

Maximum wind speed < 13 knots
Average wind speed < 10 knots
Maximum crosswind < 9 knots
Average cross wind < 6 knots

The local meteorological measurements served two important purposes: firstly, to provide a real-time assessment of the local weather prior to, and during, aircraft flight operations to ensure that prevailing conditions were within acceptable limits; and secondly, to facilitate the application of necessary post-flight corrections to the acoustic data. A layered approach to implementing weather corrections was adopted to provide accurate estimates of atmospheric absorption even in the presence of temperature inversions, which are common in the desert. In this approach, the measured temperature, relative humidity, and pressure profiles were divided into 25 ft. high layers up to 500 ft. For each layer, an average value for each variable was computed and used to correct the acoustic measurements for attenuation effects during beamforming. A detailed account of the weather measurement operation, sensors used to collect data, and the procedure for applying appropriate corrections to the acoustic data is provided in Ref. [17].

C. Phased Microphone Array

The acoustic measurements were acquired with a state-of-the-art phased microphone array developed at the NASA Langley Research Center (LaRC). The 250-foot diameter array consisted of 185 microphones arranged in a non-uniform clustering of 12 spiral arms (Fig. 6). The microphones were hardened, weather-resistant, commercial, off-the-shelf sensors integrated on circuit boards specially designed to withstand the harsh environment of Edwards AFB.

The health of the microphones was monitored during the long deployments through the use of a hovering aerial sound source and eight ground speakers that were embedded within the array pattern. Details of the array hardware, calibration, and operation are provided in Refs. [11] and [18].

Complementing the array were four "certification" microphones located around the perimeter of the array on separate tripod stands. Two of these microphones were positioned on opposite ends of the x-axis (flyover direction) and two on opposite ends of the y-axis (sideline direction) approximately 330 ft (100 m) from the array center. Measurements obtained with these microphones closely followed FAA rules and procedures. This adherence afforded the ability to determine the reduction in effective perceived noise levels (EPNL) achieved with the current NR technologies based on established procedures set by the FAA [16]. Processing and analysis of certification microphone data based on FAA guidelines is a complex and time-consuming procedure that will be deferred to a future paper.

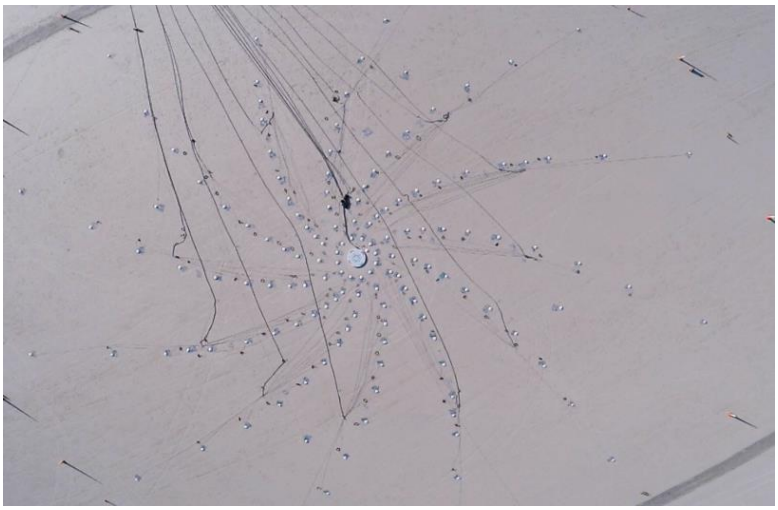

Fig. 6 Aerial view of microphone array as deployed on the lakebed at Edwards AFB.

D. Array Data Processing

Each data acquisition cycle lasted 40 seconds and was initiated when the aircraft passed a visual ground marker upstream of the array center microphone. All the microphone channels were simultaneously sampled at 76.8 kHz. The CLEAN technique, which is available within AVEC's Phased Array Software Suite [19] was used for processing the microphone array data. As a first step, beamform (source localization) maps were generated on a square, 100 ft by 100 ft (30.5 m by 30.5 m) planar grid covering the entire aircraft. Grid sizes of 101 × 101 and 201 × 201 points, representing 12 in. (30.5 cm) and 6 in. (15.25 cm) spatial resolutions, respectively, were used to ascertain spatial resolution effects on the position and sound pressure level (SPL) of the sources (see Fig. 7). The examination included narrow, $1/12^{th}$ octave band, and $1/3^{rd}$ octave band maps. In most instances, results obtained from the two grids were in close agreement. However, noticeable differences were observed for some configurations. Thus, a select number of passes were processed on a larger grid of 401 × 401 points representing a 3 in. (7.62 cm) spatial resolution. Virtually no differences were observed between the solutions extracted from the two larger grids. Therefore, only results obtained with the 6 in. resolution grid are presented in this paper. An SPL range from peak level (0 dB) to 10 dB below the peak is used for all the beamform maps included in this study.

To generate beamform maps, microphone signals were weighted (shaded) to improve the resolution at low frequencies, and to effectively reduce the array aperture size as the frequency increased, thereby minimizing the effects of decorrelation of the outer microphones in the array. Climate conditions were linearly interpolated in time from hourly aerostat measurements. Wind velocities were incorporated into the beamforming, and the atmospheric conditions were used in the absorption model of Bass et al. [20]. Atmospheric attenuation corrections were applied to each block of beamformed data using the averaged air properties within the 25 ft layers between the aircraft location (average GPS location over the data block) and the center of the array. Additionally, the results presented here were scaled to an altitude of 394 ft. (120 m) under the assumption of spherical spreading for pressure ($p'^2 \sim 1/r^2$).

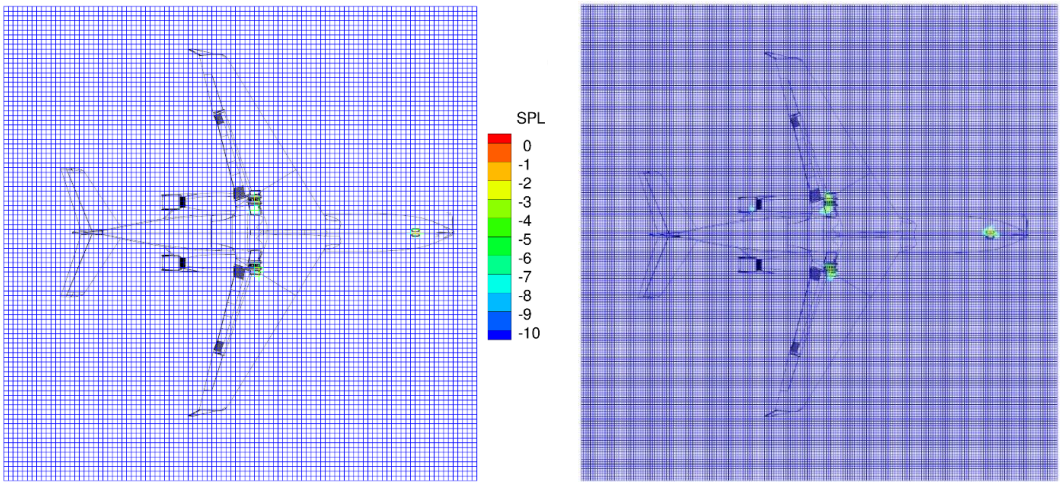

a) Standard grid of 101 × 101 points (12 in. resolution) **b) Fine grid of 201 ×201 points (6 in. resolution)**

Fig. 7 Primary grids used for computing beamform maps.

The initial beamform maps were scrutinized to isolate the primary noise sources of interest from the secondary and all other undesirable sources that are present on a real aircraft. As such, the maps are indispensable to obtain a qualitative and global view of how the NR technologies alter the intended sources. To generate the farfield spectra, the deconvolved CLEAN maps were integrated with a cutoff of 10 dB. A conventional beamform map at a frequency of 2,250 Hz is displayed in Fig. 8 for the 808 aircraft with the Fowler flaps deflected at 39º and main landing gear deployed. To isolate relative source strengths, the maximum SPL has been subtracted from all levels in the map in Fig. 8, and a range of 10 dB below the maximum has been used. This convention is also followed throughout this paper including when comparing beamform maps from different datasets: the maximum SPL within a set of maps for a given frequency is subtracted from all levels in the set, and only sources within 10 dB of the maximum are displayed.

Two integration regions were used to isolate flap and main landing gear contributions to the farfield noise and to assess the noise reduction performance of the tested technologies. These regions are highlighted in Figure 8: (1) a delta-shaped region named "WingsNg" that excludes the contributions from the nose gear, wing tips and leading edges, and engines; and (2) a small, rectangular region called "MLG" that contains the main landing gear. A third region called "Whole_AC" was used for integration of the grid containing the entire aircraft. The "WingsNg" region allowed us to examine and determine the acoustic benefits of the ACTE flap technology with and without the baseline main landing gear deployed. The "MLG" region was used to assess the isolated effectiveness of the main gear fairings and cavity treatments.

Spillage from other sources (e.g., wing tips, engine) partially contaminates the integrated noise levels for the intended airframe components, as demonstrated in Fig. 9, which depicts sample 1/12th-octave beamform maps at 265 Hz, 1,600 Hz, and 6,000 Hz for the 804 aircraft with flaps and landing gear retracted. This represents the quietest achievable configuration if the dominant airframe sources were to be totally eliminated. At low frequencies (265 Hz), the cavity associated with the fuel vapor vents near the wing tips produces a strong tonal noise that is more than 10 – 15 dB louder than any other sources on the aircraft. The map at 1,600 Hz illustrates scattering by the aircraft surfaces of the engine fan tones, which in this case appear as prominent sources at the wing leading edges. The presence of other engine-related sources is also evident in this map. At 6,000 Hz, the predominant source appears on the nacelle and is associated with the noise created by the exhaust of the bleed air used for cooling the DC generator on 804. In contrast, the 808 aircraft is equipped with an AC generator that does not require cooling, thus removing the contribution from this particular source. The integration regions introduced in Fig. 8 were devised to either remove or substantially diminish the contribution of these secondary sources to the farfield signature of the primary airframe sources of interest.

Integrated spectra from all acceptable passes for both 804 and 808 aircraft flying in the clean (flaps and landing gear retracted) configuration are plotted in Fig. 10a. The spectra were obtained from integration of the entire grid (using 10 dB cutoff) and thus represent the total noise of the aircraft. Each spectrum was computed from approximately 0.4 s time records that correspond to an aircraft position of ± 50 ft (± 15.24 m) relative to the center of the array (overhead). The broken blue lines represent 804 passes, the solid red lines correspond to 808 passes. Note that the

spectra represent multiple passes from multiple days and years[5]. Overall, good correspondence is observed between the noise generated by the two aircraft when flown in their clean (cruise) configuration. All dominant secondary sources (as highlighted in the maps of Fig. 9) appear prominently in the spectra. The corresponding spectra obtained from integrating the reduced region "WingsNg" are displayed in Fig. 10b. Recall that this region was devised to eliminate contributions from undesirable sources at the wing tips, wing leading edges, and engines. The spectra shown in Fig. 10b clearly demonstrate that our goal has not been achieved, since all secondary sources are fully identifiable. There are two main possibilities for their persistence. First, noise from these secondary sources may be reflected from various aircraft surfaces within the WingsNg region of integration. As such, their contribution to the integrated spectra is real and unavoidable. Second, the lack of dominant sources within the "WingsNg" region causes the integration process to yield only the contribution from the side lobes associated with the secondary sources. In either scenario, determination of the full acoustic performance of some noise reduction technologies becomes exceedingly difficult, especially at frequencies below 300 Hz and above 5 kHz.

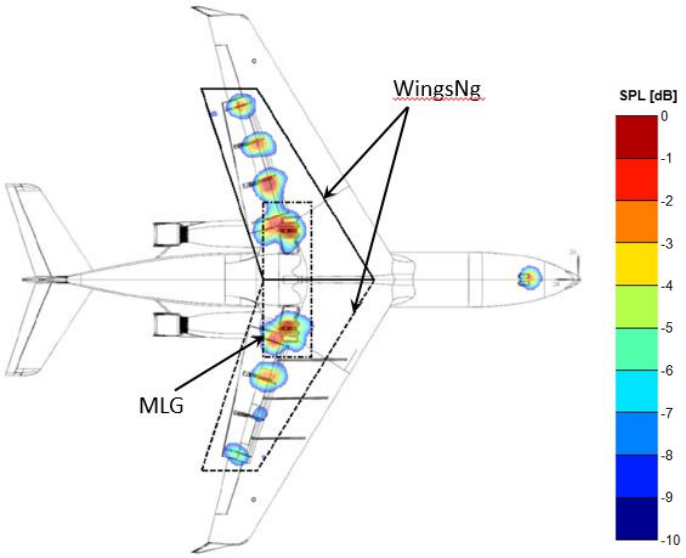

Fig. 8 Primary integration regions used to include or exclude contributions of measured sources to the farfield noise spectrum. A sample acoustic map using conventional beamforming is shown.

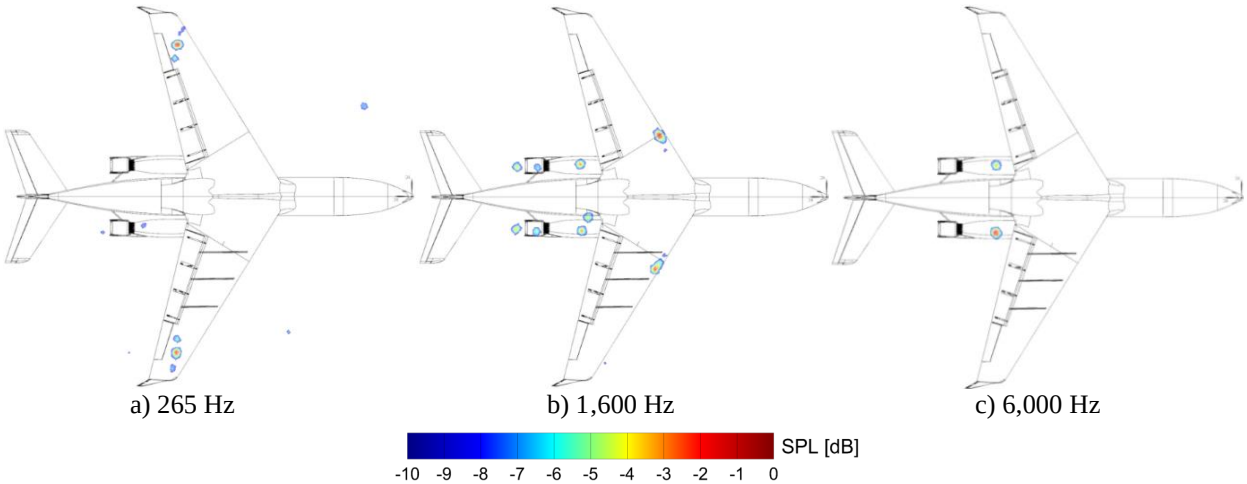

a) 265 Hz b) 1,600 Hz c) 6,000 Hz

Fig. 9 CLEAN beamform maps at low-, mid-, and high-frequency for 804 aircraft with flaps and landing gear retracted.

[5] The legend for each spectrum includes date, pass number, integration region, and airspeed. Although identification of a large number of passes in any given figure may reduce clarity, the legends were included to demonstrate temporal repeatability of the measured data.

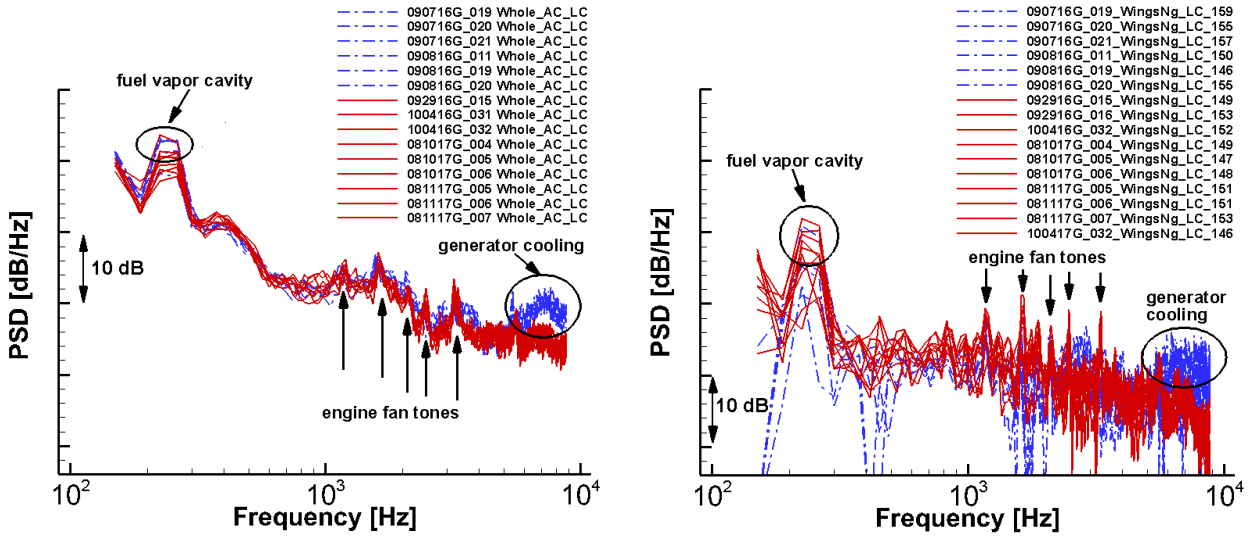

a) whole aircraft region **b) WingsNG region**

Fig. 10 Integrated spectra from 804 and 808 passes over array for the configuration with flaps and landing gear retracted.

E. Background Noise

The background noise signature at the test site plays a key role in the quality of the measured airframe noise signatures by setting the signal-to-noise ratio (SNR) during data acquisition. Background noise was measured several times during the course of the tests when the aircraft was far away from the microphone array. A sample background noise measurement is shown in Fig. 11. Also presented on the same figure are the uncorrected power spectral density (PSD) plots from the array center microphone obtained during aircraft flyovers on September 29, 2016 (pass number 008) and October 4, 2016 (pass number 018). The data were processed in narrow band with a bin width of 37.5 Hz. Note that the background noise is highest at frequencies below 1 kHz because of road noise from a nearby highway; at higher frequencies, the background noise plateaus because the noise floor of the system (microphones, amplifiers, filters, and data acquisition system) was reached. As can be seen from Fig. 11, a good SNR was maintained for sound waves with frequencies less than 5 kHz – 6 kHz. Atmospheric attenuation of high-frequency noise, especially during "bad" or "marginal" days, degraded the SNR for frequencies above 6 kHz. The combination of background noise, atmospheric attenuation of high-frequency waves, and the presence of residual engine noise rendered airframe noise signals extracted from the high-frequency segment of the spectrum questionable at best. As a result, we restrict our discussions of integrated spectra to frequencies below 6 kHz.

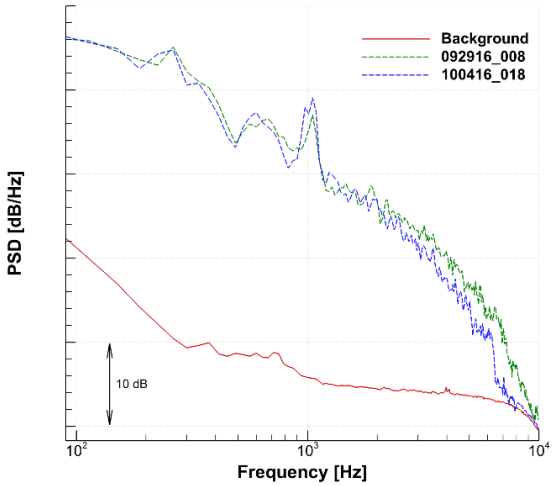

Fig. 11 Sample background noise levels at the microphone array site.

IV. Results and Discussion

To determine velocity scaling and other dependencies of airframe noise, measurements were conducted at 140, 150, and 165 kts, with multiple passes at each speed to improve the statistical quality of the collected data. However, the majority of the passes were conducted at the nominal speed of 150 knots that is close to, and representative of, typical aircraft landing speeds. The highest-quality acoustic results were obtained from the period corresponding to the streamwise segment ± 50 ft from the array center (overhead position), when the aircraft was closest to the array microphones, and, thus, atmospheric attenuation or wind-caused decorrelation of high-frequency sound were at their lowest. Therefore, unless specified otherwise, all results presented here correspond to the overhead position.

A. Evaluation of ACTE Flap Technology

The 2016 test campaign focused on the aeroacoustic evaluation of the ACTE flap technology. Although other deflection angles were evaluated, the ACTE flap 25° was the most heavily tested configuration. This configuration was reevaluated during the 2017 campaign to determine data repeatability over multiple years.

The aerodynamic data collected were limited to steady surface pressure measurements at three streamwise rows along the span of the port wing. Measured steady surface pressure coefficient (C_p) distributions at two spanwise locations for the 804 aircraft with ACTE flaps at 25º are shown in Figure 12. The data correspond to multiple passes with closely-matched, recorded aircraft AOA from two different flights. The passes were performed at different speeds with landing gear retracted (gear up) and deployed (gear down). Notice the excellent data repeatability achieved with the 804 aircraft, which is a direct result of the extensive pretest preparations and precision flying of the NASA AFRC test pilots. Also note that the curves have continuous surface pressure distributions, as is typical of single-element wing sections. This characteristic stems from the seamless integration of the ACTE flap technology into the wing design.

Sample CLEAN 1/12th octave beamform maps for 808 with its Fowler flaps deflected at 39º and 804 with ACTE flaps set at 25º, with the landing gear retracted, are presented in Figure 13 for a frequency of 1,725 Hz. Peak SPL for the two maps are within 0.9 dB of each other. As expected for the 808 aircraft, the primary noise sources associated with the Fowler flaps reside at the inboard and outboard side edges, with the flap brackets acting as prominent secondary sources. In contrast, the ACTE technology totally removes these noise sources because it eliminates the flap side edges and the flap bracket assemblies; as a result, only engine noise appears in the map. The corresponding maps with landing gear deployed are shown in Figure 14. For these maps, peak SPL are within 0.2 dB of each other. For the 808 (baseline) aircraft, the landing gears (particularly MLG) show up as the most dominant sources. Flap noise also appears in the map, however, attesting to the importance of this component relative to the landing gear. With the ACTE technology applied, only the landing gears appear in the map, indicating that flap noise is at least 10 dB below the gear levels at this frequency.

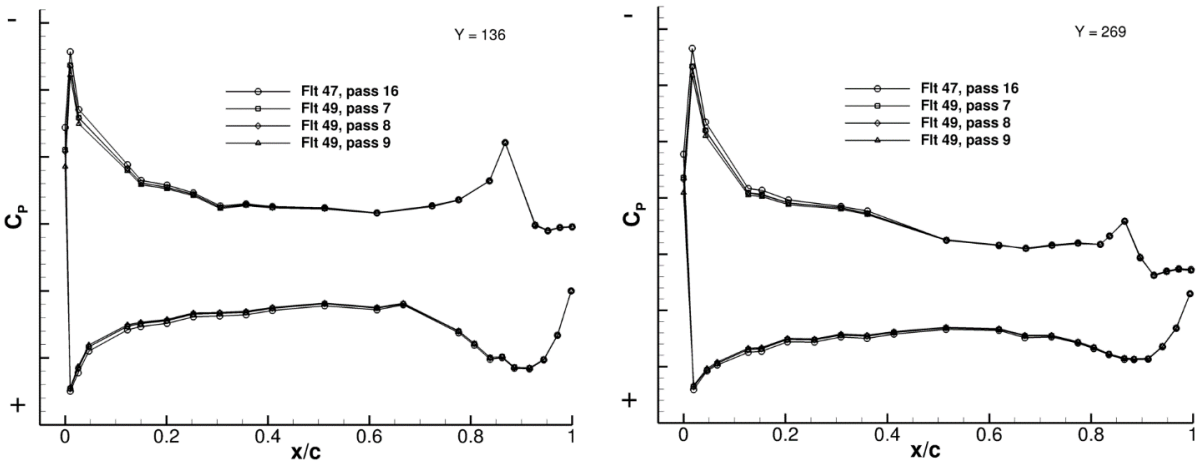

Figure 12. Streamwise steady surface pressure distributions at spanwise locations of 136 in and 269 in, 804 aircraft with ACTE flaps deflected at 25º.

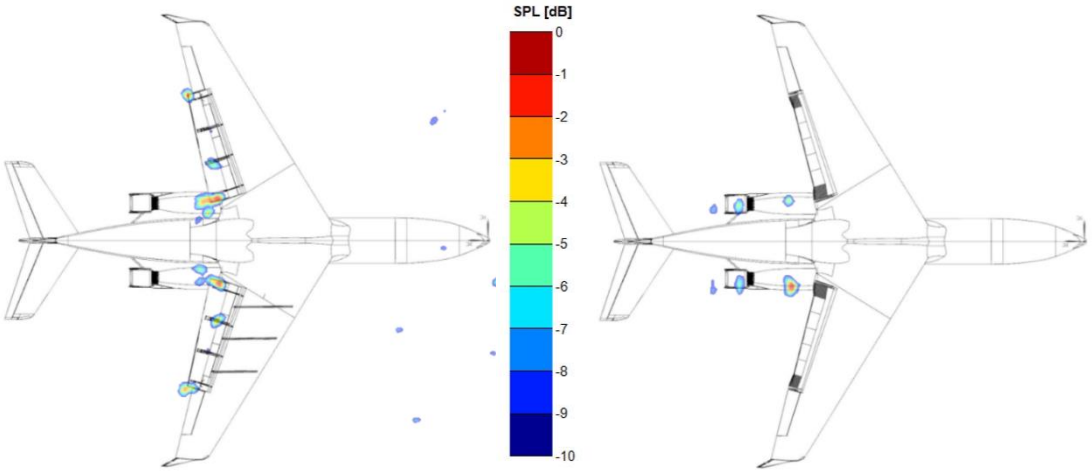

a) 808 with Fowler flaps at 39º **b) 804 with ACTE flaps at 25º**

Figure 13. Noise produced by Fowler and ACTE flaps with landing gear retracted, f = 1,725 Hz.

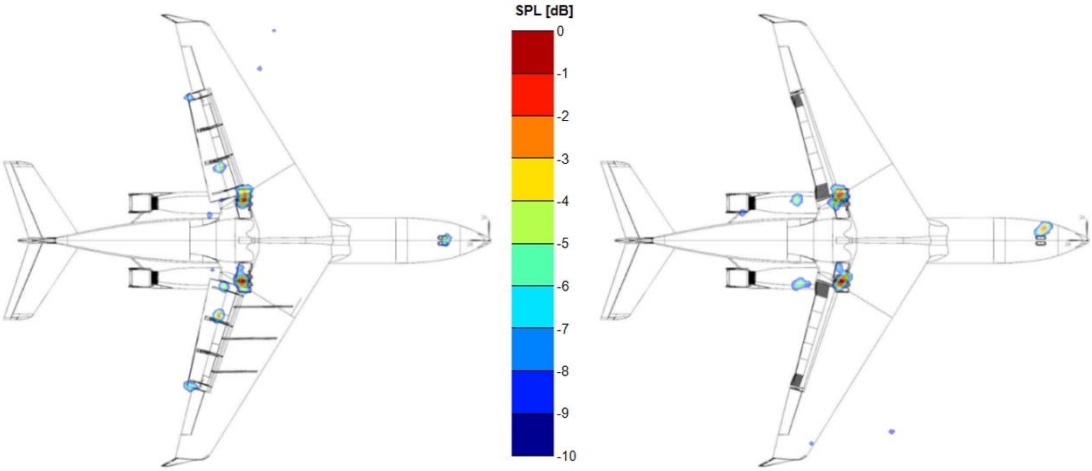

a) 808 with Fowler flaps at 39º **b) 804 with ACTE flaps at 25º**

Figure 14. Noise produced by Fowler and ACTE flaps with landing gear deployed, f = 1,725 Hz.

The pertinent velocity scaling for the noise generated by the aircraft flaps and main landing gear is exemplified in Fig. 15 using the 808 with a flap deflection of 39° and gear deployed. Plotted in Fig. 15a are the integrated spectra from the "WingsNg" region at three speeds. The strong tone centered around 970 Hz in the spectrum for 148 knots was generated at the main gear knee joint by the hollow front post. The tone is absent from the spectra for the lower and higher speeds. Scrutiny of other passes for this configuration revealed that the tone is mostly present within the aircraft speed range of 150 kts ± 6 kts. However, even at speeds close to 150 kts, depending on wind direction and the magnitude of the cross wind, the tone could be absent from both sides of the MLG or present on one side only. The nominal speed of V_{ref} = 150 kts was used to normalize all spectra according to the sixth power (V^6) scaling law. The normalized spectra are presented in Fig. 15b. Excellent collapse of the measured spectra is observed, highlighting the dominance of flap and gear sources within the 'WingsNg" integration region. We note here that the best data collapse was achieved without applying any scaling to the frequencies. For the remainder of the paper, spectral results will be presented based on V^6 normalization using V_{ref} = 150 kts.

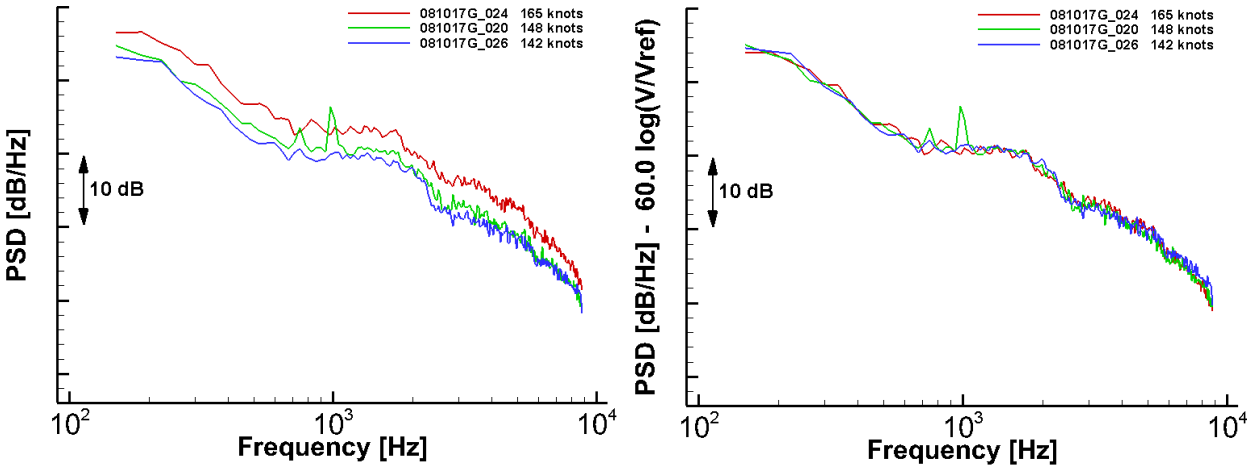

a) unscaled **a) scaled**

Fig. 15 Spectra from 808 passes for flap 39°, gear deployed configuration prior (left) and after (right) applying V^6 scaling. No Strouhal scaling has been applied to frequencies.

To illustrate the repeatability and statistical quality of the measured spectra, we revert to the configuration with ACTE flap 25° and gear deployed. Since this was the most tested configuration, the corresponding sample pool is large. In Fig. 16a, we present "all" the acceptable passes collected during days marked with "good", "marginal", and "bad" weather conditions. Altogether, the passes encompass six different flights/dates from the 2016 and 2017 test campaigns. The thick solid black line represents the averaged spectrum based on p^2 averaging. Notice that there is good data repeatability, especially at frequencies below 3 kHz. The spread in levels is between 2 dB to 3 dB for frequencies below 2 kHz, gradually increasing to 4.5 dB at 6 kHz. The larger spread in levels at higher frequencies is mainly due to severe atmospheric attenuation during bad weather days that causes degradation in the SNR [16]. To demonstrate this problem, we have replotted in Fig. 16b only the spectra from those passes that were obtained on "good" and "marginal" days – a marked improvement in the tightness of the spread among the various passes is apparent. This grouping of spectra is termed as "select" passes. Five of the passes with closely-matched aircraft TAS, AOA, weight, and position over the array are replotted in Fig. 16c. This grouping, which is identified as "best matched" passes, provides the tightest collapse of the spectra, indicating that excellent data repeatability can be achieved if one can keep aircraft and test conditions within a narrow range for several flights. The averaged spectrum from each group of passes shown in Figs. 16 a-c is plotted in Fig. 16d. The largest differences occur between averaged spectra from "all" and "best matched" passes, which are less than 0.5 dB over the frequency range below 6 kHz. The differences between the averaged spectra from the "select" and "best matched" passes are even smaller and typically fall below 0.3 dB. The spectra from acceptable passes for the 808 aircraft configurations of flap 20° and 39° with landing gear retracted and deployed are presented in Fig. 17. These correspond to some of the baseline configurations used to evaluate the acoustic performance of the flap and MLG NR technologies. As can be seen, similar spreads to those observed for the 804 spectra are apparent, despite the fact that the spectra were normalized by the IAS due to unavailability of the TAS for the 808 aircraft. We are confident that a tighter collapse would have been achieved had normalization been done using TAS. The integrated spectra for all other tested configurations show similar trends with regard to pass repeatability. Therefore, for clarity, we will mostly rely on averaged spectra to discuss spectral content, levels, and features for the various aircraft configurations that were flight tested.

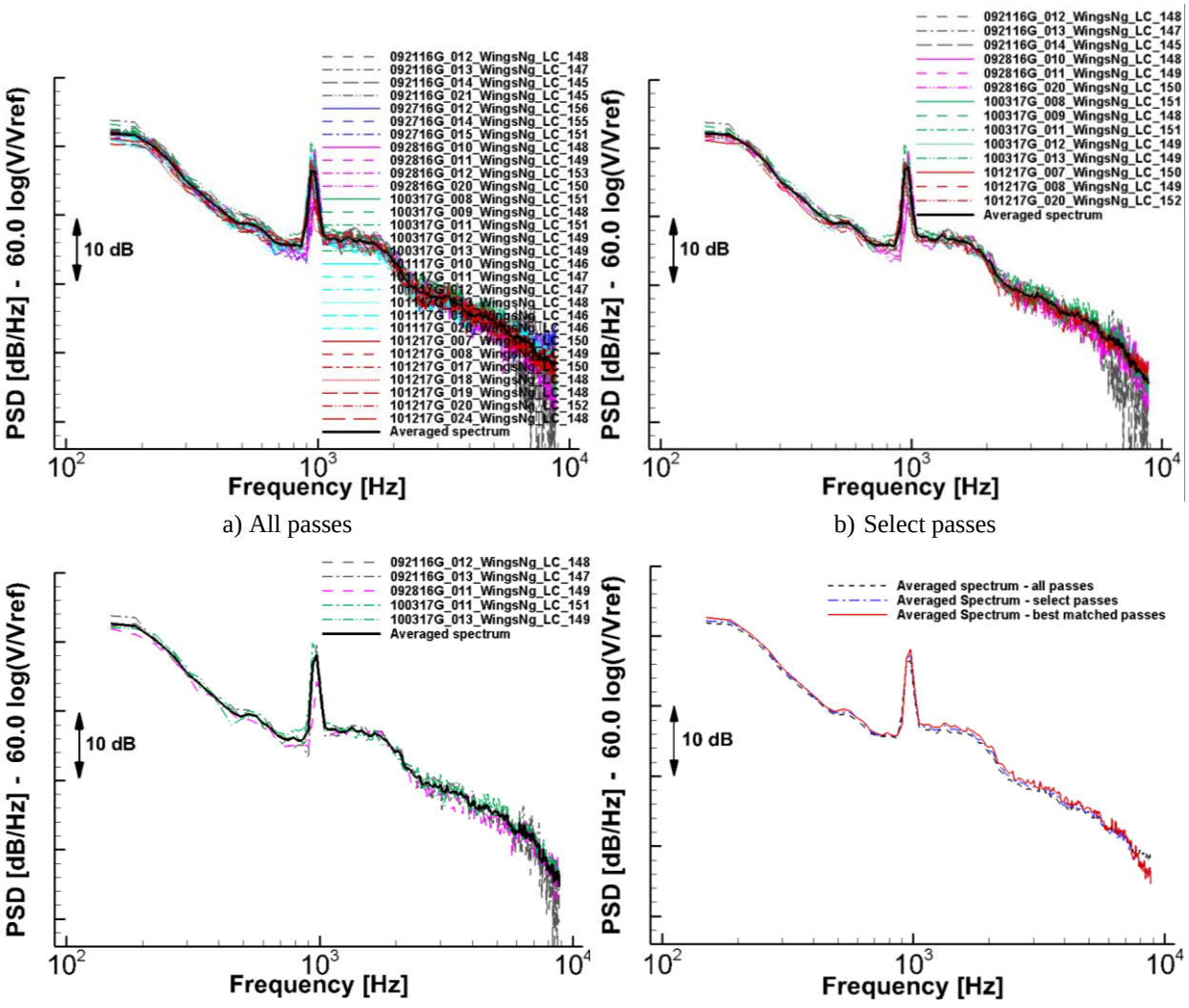

a) All passes b) Select passes

c) Best matched passes d) Averaged

Fig. 16 Spectra from 804 passes for configuration with ACTE flap 25°, landing gear deployed.

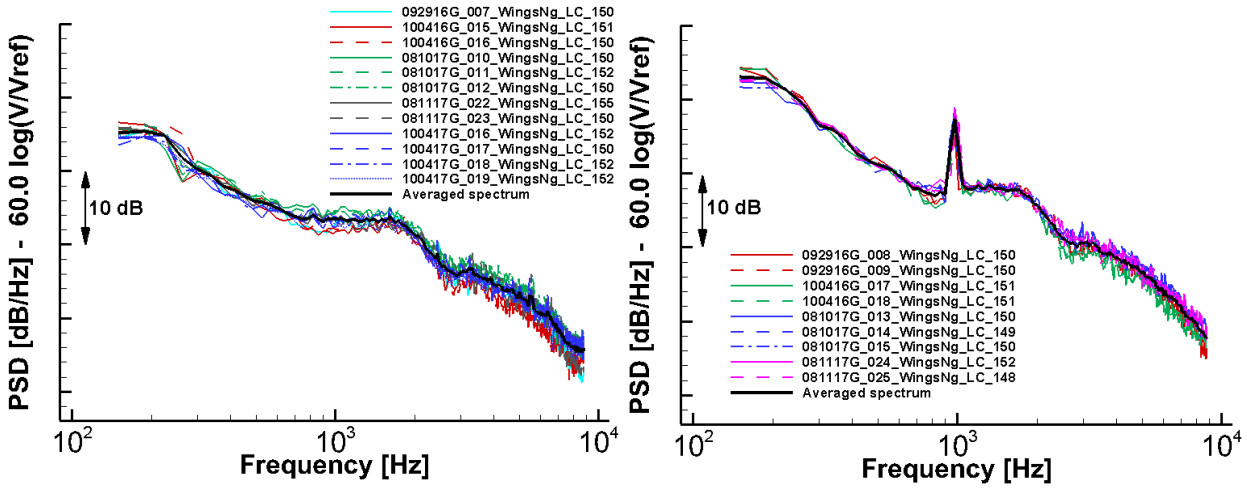

a) flap 20°, gear retracted b) flap 20°, gear deployed

Fig. 17 Collected spectra from 808 passes for flaps 20° and 39° with landing gear retracted and deployed.

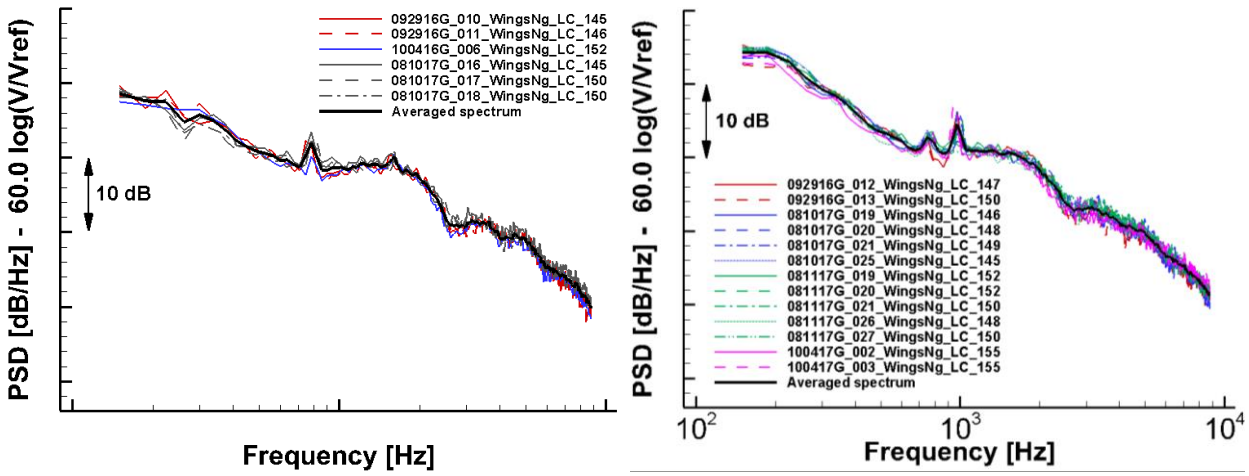

c) flap 39°, gear retracted

d) flap 39°, gear deployed

Fig. 17 Concluded.

Component-level contributions from the Fowler flaps and MLG to the farfield noise signature of 808 are shown in Fig. 18. The integrated averaged spectra were obtained from summation of the sources within the "WingsNg" region. Relative to the cruise configuration (flap 0°, gear retracted), the MLG contribution falls within the levels produced by the Fowler flaps deflected at 20° and 39°, except for frequencies below 400 Hz. Recall that the integrated results for flap 0°, gear retracted are likely contaminated by dominant sources outside the "WingsNg" region. At low frequencies, noise from the MLG wheel cavity dominates the spectra by a large margin. When both components are deployed, close proximity of the main gear to the inboard edge of the flap causes interaction (installation) effects that may dominate the farfield acoustic signature, making it virtually impossible to isolate individual contributions.

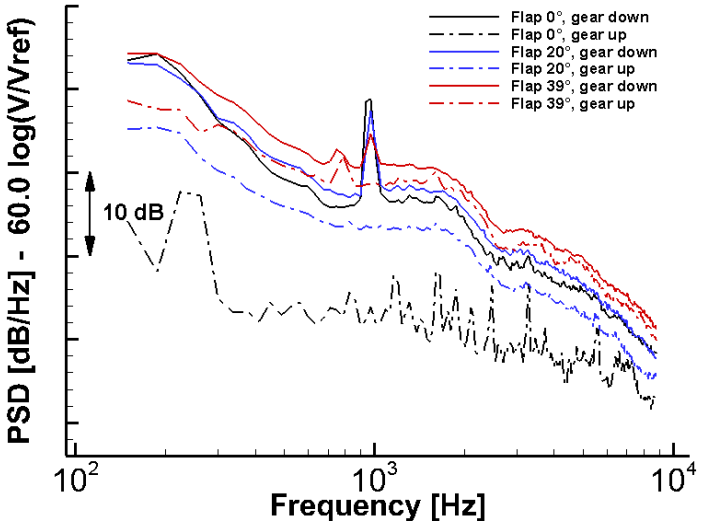

Fig. 18 Individual and combined contributions of Fowler flap and MLG components to farfield noise at different flap deflections. Averaged spectra are from 808 passes.

Acoustic performance of the ACTE technology, relative to the baseline Fowler flap, is best illustrated by the integrated noise spectra presented in Fig. 19. The plots presented in Fig. 19a compare the noise signature of the ACTE and Fowler flaps for their respective two highest flap deflections tested without landing gear deployed. The spectrum for ACTE flap 0° is included for reference purposes. As inferred from the data presented in Fig. 10a, both flap systems produce similar noise levels when retracted. The integrated spectra corroborate the trends observed in the beamform maps of Fig. 13 and 14. The integrated spectra demonstrate that the ACTE technology reduces flap noise by nearly 10 dB over the entire frequency range, virtually eliminating the contribution from this component. Similar behavior was observed at other directivity angles forward of 90° (overhead). Inspection of the beamform maps revealed that

the low-frequency, broad tonal hump seen in the ACTE spectra is residual noise from the wing tip fuel vapor vents and other sources on the engine nacelles. As mentioned previously, the degradation in ACTE acoustic performance at frequencies above 4 kHz is attributed to several factors beyond our control, foremost among them low SNR, residual engine noise, and background noise. The near-total elimination of flap noise is illustrated in Fig. 19b, where the effect of gear deployment at various ACTE flap deflections is shown. Notice that all spectra are within a very narrow spread, indicating that the noise signature is dominated by the MLG. In contrast, observe from the spectra of Fig. 18 that, even with MLG deployed, significantly more noise is produced with increasing Fowler flap deflections.

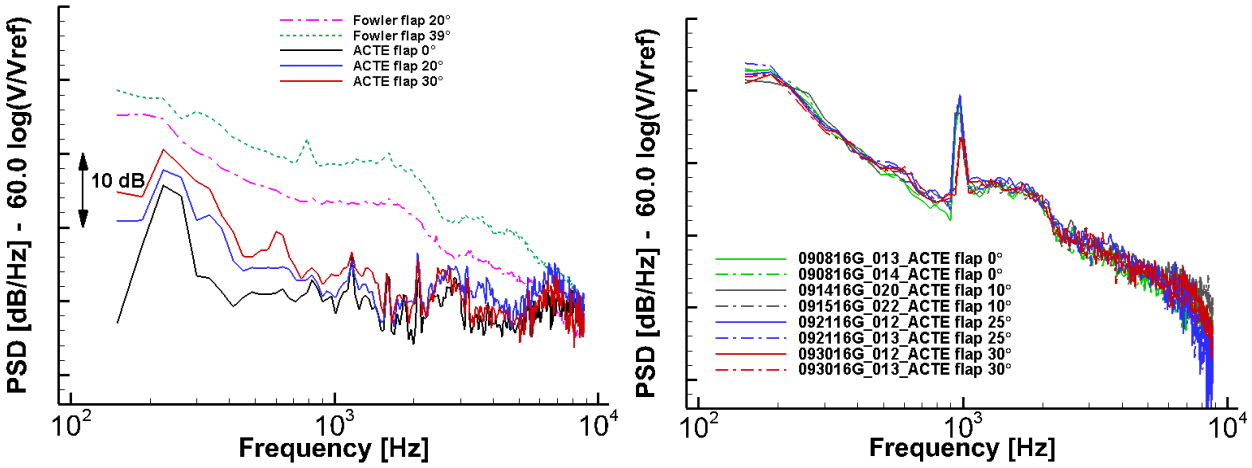

a) ACTE vs. Fowler flap, gear retracted **b) ACTE with main gear deployed**

Figure 19. Integrated farfield noise spectra produced by Fowler and ACTE flaps with landing gear retracted and deployed.

B. Evaluation of MLG and Cavity NR Technologies

The 2017 flight test campaign focused on the aeroacoustic evaluation of the MLG NR technologies. The gear fairings plus the cavity treatments were tested on the 804 aircraft equipped with the ACTE flaps. The flaps were set at a deflection of 25° for all flights, except an initial flight conducted with flaps at 0°. Determination of the full acoustic performance of various combinations of the MLG noise abatement technologies was vastly improved through the virtual elimination of flap noise afforded by the ACTE system.

Sample 1/3rd octave beamform maps for the 804 aircraft without and with landing gear and cavity treatments are presented in Fig. 20 for three frequencies representative of low-, mid-, and high-frequency segments of the noise spectrum. The images correspond to the absence (left column) or presence (right column) of gear treatments. The treated configuration shown represents the combination of landing gear fairings, chevrons, and sound absorbing foam for the cavity. The maximum SPL for the maps on each row were very similar; thus, a direct comparison between each pair of images provides the magnitude of the reduction levels. As indicated earlier (Fig. 18), the low frequency segment of the noise spectrum is dominated by the main gear cavity. Figure 20b provides clear evidence that application of chevrons and foam to the gear cavity is highly effective, resulting in substantial noise reduction. In the mid- to high-frequency ranges (Figs. 20c through 20f), the MLG fairings provide significant noise reduction benefits. Although not shown, similar levels of noise reduction were observed at other frequencies.

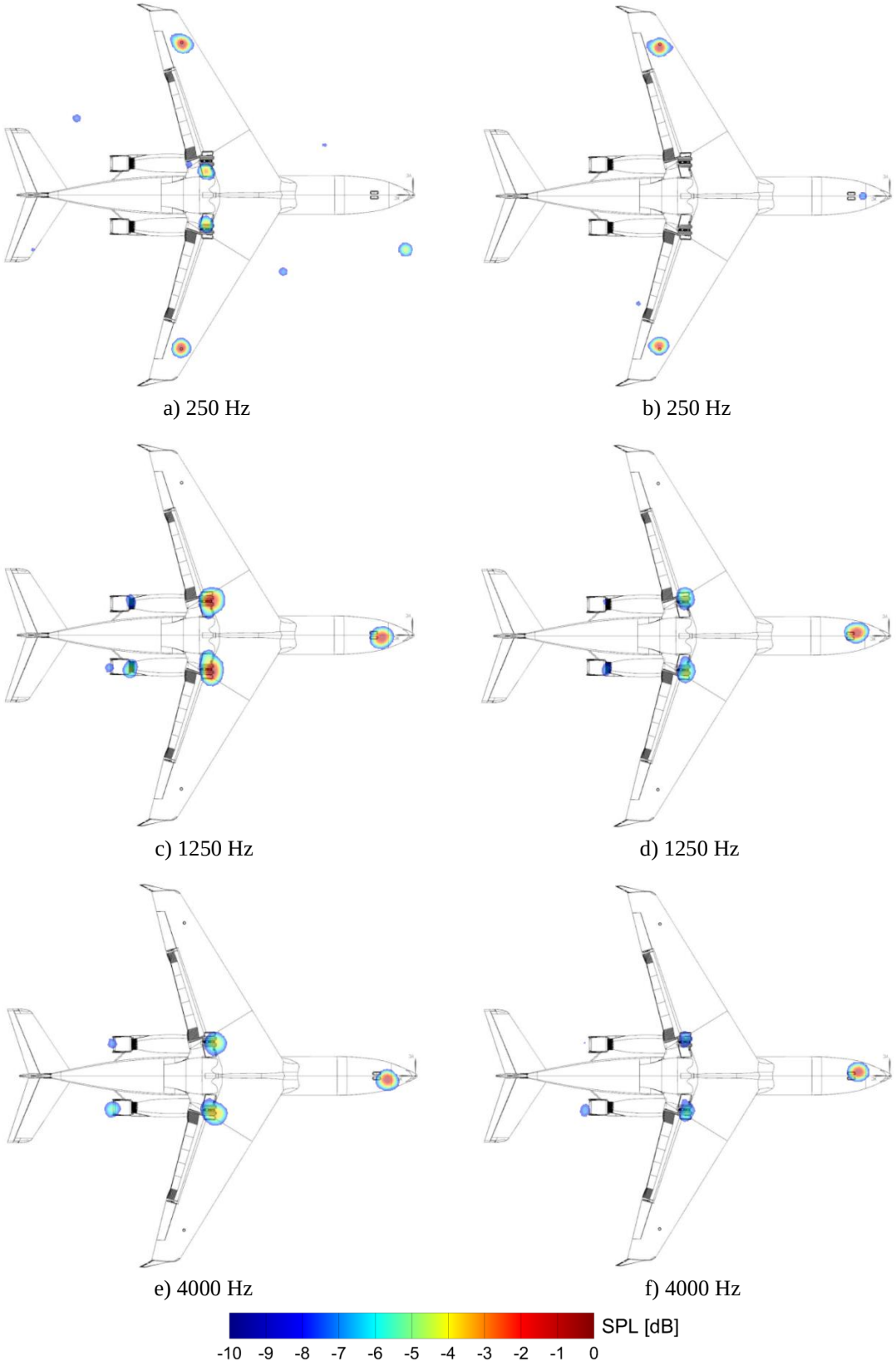

Fig. 20 Noise produced by ACTE-equipped 804 without (left column) and with (right column) NR technologies installed on MLG and cavity. ACTE flaps deflected at 25°.

To accurately extract the noise reduction attained with the MLG technologies, we switched to the "MLG" region for integrating the CLEAN beamform maps. To illustrate the benefits of this switch, the integrated spectra obtained from the "WingsNg" and "MLG" regions for the configuration with ACTE flap 25° and gear deployed are shown in Fig. 21a. For frequencies up to 2 kHz, the two regions produce very similar spectra, with the "WingsNg" region having slightly higher levels (on the order of 0.3 dB) due to the larger area of the integrand. The closeness of the two spectra indicates, again, that the ACTE flaps produce very little noise. The spectrum from the "WingsNg" region shows higher noise levels above 2 kHz, mainly due to contamination from residual engine noise. Corresponding results for the period when the aircraft is between 300 ft and 200 ft forward of the array center (~55° directivity angle) are shown in Fig. 21b. Similar spectral behavior is observed, indicating that the trends are not directivity-dependent.

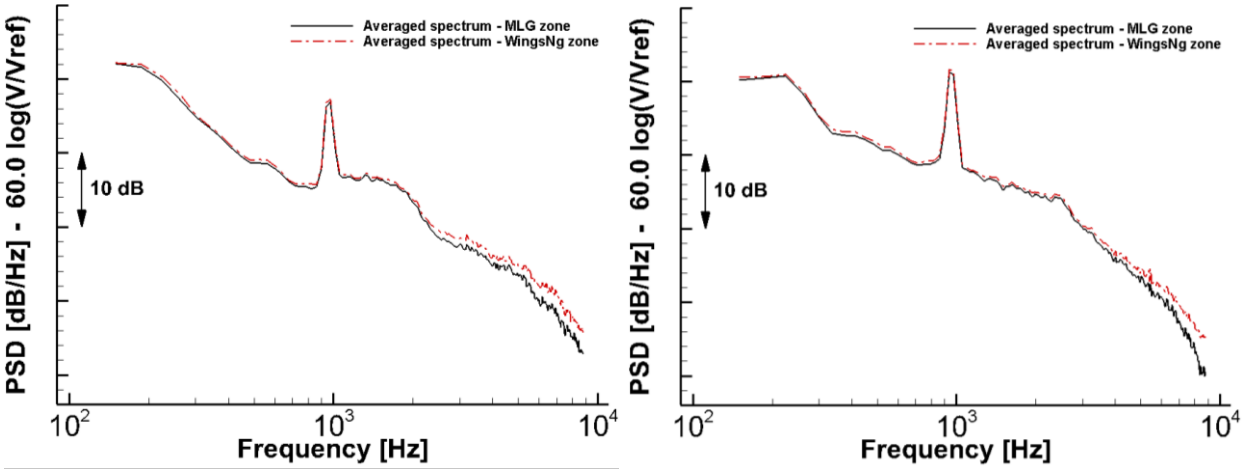

a) overhead position (90° directivity angle) b) 300 ft forward of array center (~55° directivity angle)

Fig. 21 Differences in integrated spectra between "MLG" and "WingsNg" integration regions for two directivity angles.

Integrated spectra for all tested combinations of the MLG fairings and cavity treatments are presented in Figs. 22a-22d. Results are shown for aircraft positions of ±50 ft (±15 m), -200 ft to -100 ft (-61 to 30 m), -300 ft to -200 ft (-91 to -61 m), and -400 ft to -300 ft (-122 to -91 m) relative to the array center. These positions correspond, approximately, to forward directivity angles of 90º, 67º, 55º, and 45º, respectively. The configuration with the MLG fairings in isolation performs well, providing close to 2 – 3 dB reduction in the 500 Hz – 5 kHz frequency range. The fairings provide measurable reduction below 500 Hz. The full extent of the reduction, however, is partially masked by the dominant wheel-well cavity noise. The noise reduction trends hold over a large range of forward emission angles where the contribution of airframe noise peaks, indicating that the benefits would translate into lower EPNLs. The gradual, diminishing performance of the MLG fairings at frequencies above 3 kHz (especially at the smaller directivity angles) is solely caused by the simultaneous effects of residual engine noise and degradation in the SNR, as the sound waves have to propagate over larger distances. As expected, the addition of the cavity mesh provides significant additional reduction, on the order of 2 dB, at frequencies below 300 Hz. However, based on the large-scale wind tunnel results of Ref. [5], we had anticipated slightly better performance from the mesh concept. This underperformance can be attributed partially to the size (diameter) of the mesh threads, which did not correspond exactly to the scaled-up size of the threads used in Ref. [5]. Note that when overhead (Fig. 22a), the mesh produces more noise than the baseline (untreated) configuration at frequencies above 4 kHz. The self-generated noise is most likely related to small-scale turbulence (e.g., vortex shedding) by the mesh threads radiating in a direction normal to the mesh plane (overhead). The quietest aircraft configuration was achieved by combining the MLG fairings with the cavity chevrons plus sound absorbing foam. Addition of this cavity treatment significantly diminished cavity noise by 4 – 5 dB at frequencies below 400 Hz. This level of performance was maintained at all directivity angles examined. Acoustic benefits were observed at frequencies as high as 3 kHz.

While a more definitive measurement of the total noise reduction gains for the treated configurations relative to the 804 aircraft equipped with Fowler flaps (baseline) has to wait until the 2018 test data are processed, a preliminary assessment can be made using available 808 data. This was accomplished by comparing the results obtained for 804 with ACTE flap 25º, MLG fairings, and cavity chevrons and foam to those for the 808 aircraft with Fowler flaps

deflected at 39º, gear deployed. Sample beamform maps at 1,250 Hz are shown in Fig. 23. The contrast between the two configurations is striking: the noise sources associated with the Fowler flap system are gone and a significant reduction in MLG noise was obtained. The integrated spectra for the quietest 804 configuration vs. 808 at its two highest Fowler flap deflections are presented in Fig. 24. The spectra clearly illustrate that a substantial reduction in noise was achieved with the installed treatments.

Evaluation of the acoustic performance of the MLG NR technologies as installed in 804 with its original Fowler flap system is the last remaining step. A main objective of the flight test campaign executed during the Spring of 2018 was to explore and address this issue. Post-processing and analysis of the 2018 test data are ongoing and the results will be published in the near future.

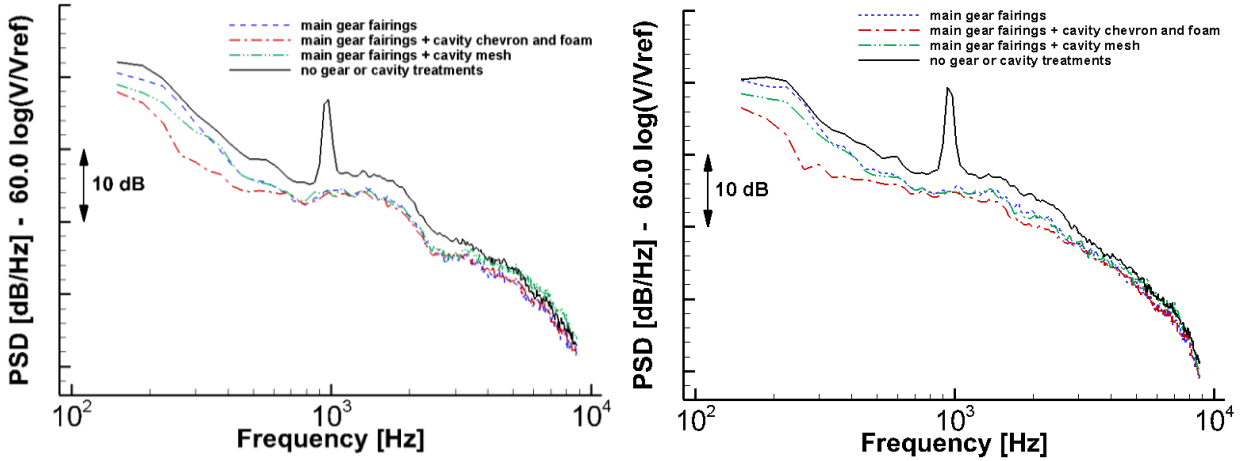

a) ±50 ft

b) -200 ft to -100 ft

c) -300 ft to -200 ft

d) -400 ft to -300 ft

Fig. 22 Integrated spectra based on "MLG" region for tested combinations of MLG fairings and cavity treatments at four aircraft positions relative to the array center. ACTE flaps deflected 25º.

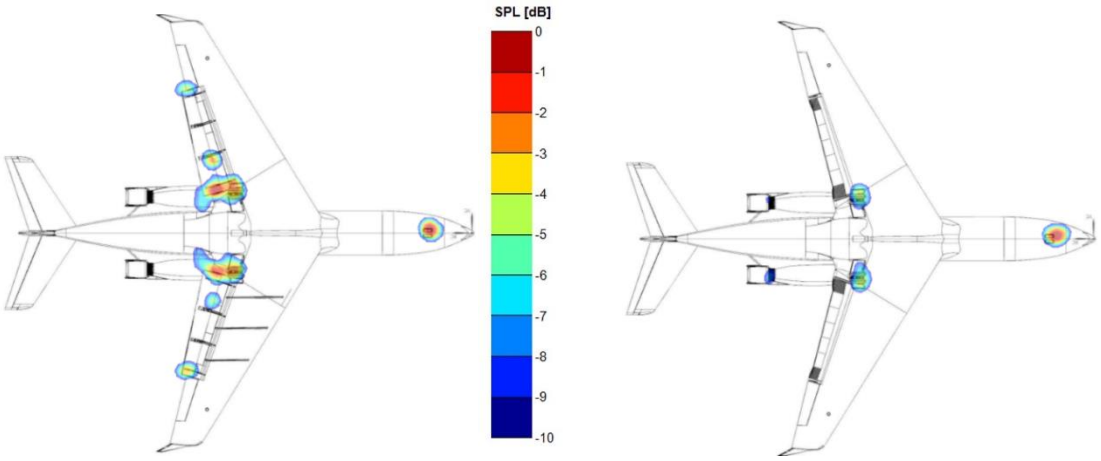

a) 808, flaps 39º, gear deployed b) 804, ACTE flaps 25º, MLG fairings, cavity chevrons and foam

Fig. 23 Comparison between 808 and 804 aircraft depicting noise reduction performance of installed technologies at 1,250 Hz.

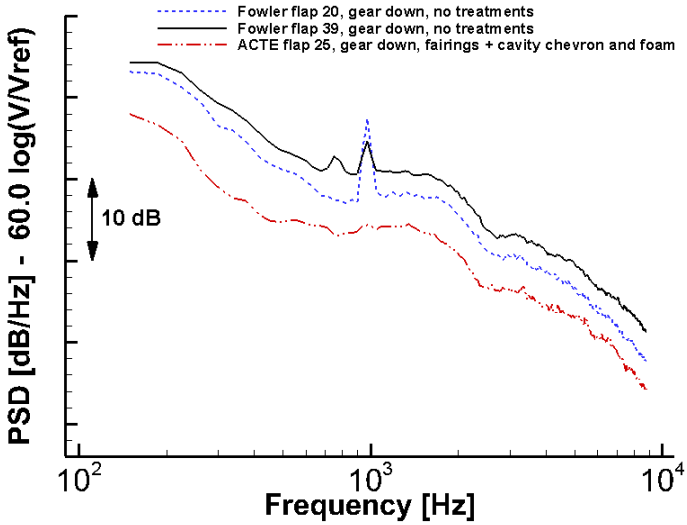

Fig. 24 Integrated spectra for 804 in its quietest configuration vs. 808 at its two highest flap deflections.

V. Concluding Remarks

A series of three flight tests focused on flap and main landing gear noise abatement technologies was planned and successfully executed under the NASA Flight Demonstrations and Capabilities project. The primary goals of the tests were to evaluate the aeroacoustic performance of several noise reduction technologies in a relevant environment and to acquire a comprehensive, high-quality database for validation of the state of the art in simulation-based airframe noise prediction methodologies. The tested technologies – an Adaptive Compliant Trailing Edge (ACTE) flap, main landing gear (MLG) fairings, and gear cavity treatments – were integrated on a NASA Gulfstream G-III aircraft to determine their effectiveness on component-level (individually) and system-level (combined) bases. A second, unmodified G-III aircraft was used also as a testbed for gathering baseline acoustic data.

The ACTE flap was evaluated during the first and second flight tests, conducted during August-October of 2016 and August-October of 2017, respectively, at Edwards Air Force Base in California. With the aircraft flying an approach pattern and the engines set at ground idle, extensive acoustic measurements were obtained using a phased microphone array system. The acquired data comprise a vast number of aircraft passes executed during numerous flights. The large, comprehensive sets of data obtained ensure that statistically meaningful trends can be discerned from the beamform maps and corresponding integrated spectra. Thus, pass-to-pass, day-to-day, and year-to-year repeatability of the acoustic measurements was analyzed and evaluated. Dependent on local weather conditions during

a given test day, good data repeatability was attained with a 2 dB spread among the various integrated spectra for most configurations of interest. The measured data clearly demonstrate that the ACTE technology drastically reduces the noise associated with the baseline Fowler flap system by more than 10 dB, virtually eliminating the contribution to farfield airframe noise from this prominent source.

The MLG and cavity noise reduction technologies were evaluated during the second flight test (August-October 2017). These technologies were installed on the main landing gear of the G-III aircraft equipped with the ACTE flaps. Elimination of flap noise permitted a highly-accurate determination of the noise reduction levels achieved with the landing gear technologies. The MLG fairings reduced the noise levels for this component by 2 – 3 dB across most of the frequency range of interest. Simultaneous application of the cavity mesh and gear fairings further reduced the low-frequency component of the farfield spectrum dominated by wheel cavity noise. The combination of MLG fairings, cavity chevrons, and sound-absorbing foam reduced low-frequency noise levels by 4 – 5 dB, drastically lowering cavity noise. Unexpectedly, the integrated spectra showed that the cavity chevrons plus foam treatment reduced main gear noise over a large frequency range that extends to 3 kHz.

The third flight test campaign was executed during March-May of 2018 and focused on the evaluation of the aforementioned gear technologies on the G-III equipped with its original Fowler flaps. Post-processing of the gathered data is ongoing and will be reported in the near future.

Acknowledgments

This work was supported by the Flight Demonstrations and Capabilities (FDC) project under the Integrated Aviation Systems Program (IASP) of the NASA Aeronautics Research Mission Directorate. These flight tests would not have been possible without the dedicated effort of a large group of people, especially the NASA Armstrong Flight Research Center personnel. In particular, we would like to express our sincere appreciation to Ethan Bauman (SCRAT Chief Engineer), Erin Waggoner, and the lead test pilots Timothy Williams and Troy Asher.

References

[1] Adib, M., Catalano, F., et al., "Novel Aircraft-Noise Technology Review and Medium- and Long-Term Noise Reduction Goals," International Civil Aviation Organization, Doc. 10017, 2014.

[2] https://www.faa.gov/data_research/aviation/aerospace_forecasts/media/FY2016-36_FAA_Aerospace_Forecast.pdf, accessed October 24, 2016.

[3] Dobrzynski, W., "Almost 40 Years of Airframe Noise Research: What Did We Achieve," *J. Aircraft*, Vol. 47, No. 2, March-April 2010, pp. 353–367.

[4] Horne, W. C., James, K. D., Arledge, T. K., Soderman, P. T., Burnside, N., and Jaeger, S. M., "Measurements of 26%-scale 777 Airframe Noise in the NASA Ames 40- by 80 Foot Wind Tunnel," AIAA Paper 2005-2810, May 2005.

[5] Khorrami, M. R., Humphreys, W. M. Jr., Lockard, D. P., and Ravetta, P. A., "Aeroacoustic Evaluaion of Flap and Landing Gear Reduction Concepts," AIAA Paper 2014-2478, June 2014.

[6] Fares, E., and Casalino, D., and Khorrami, M. R., "Evaluation of Airframe Noise Reduction Concepts via Simulations using a Lattice-Boltzmann Approach," AIAA Paper 2015-2988, June 2015.

[7] Khorrami, M. R., Fares, E., Duda, B., and Hazir, A., "Computational Evaluation of Airframe Noise Reduction Concepts at Full Scale," AIAA Paper 2016-2711, May-June 2016.

[8] Piet, J. F, Davy, R., Elias, G., Siller, H. A., Chow, L.C., Seror, C., and Laporte, F., "Flight Test Investigation of Add-On Treatments to Reduce Aircraft Airframe Noise," AIAA Paper 2005-3007, May 2005.

[9] Elkoby, R., Brusniak, L., Stoker, R., Khorrami, M. R., Abeysinghe, A., and Moe, J.W., "Airframe Noise Results from the QTD II Flight Test Program," AIAA Paper 2007-3457, May 2007.

[10] Yamamoto, K., Takaishi, T., Murayama, M., Yokokawa, Y., Ito, Y., et al., "FQUROH: A Flight Demonstration Project for Airframe Noise Reduction Technology – the 1st Flight Demonstration," AIAA Paper 2017-4029, June 2017.

[11] Humphreys, W. M. Jr., Lockard, D. P., Khorrami, M. R., Culliton, W. G., McSwain, R. G., Ravetta, P. A., and Johns, Z., "Development and Calibration of a Field-Deployable Microphone Phased Array for Propulsion and Airframe Noise Flyover Measurements," AIAA Paper 2016-2898, May-June 2016.

[12] Baumann, E. and Waggoner, E., "Flight and Ground Operations in Support of Airframe Noise Reduction Test," Paper to be presented at the AIAA/CEAS Aeroacoustics Conference in Atlanta, Georgia, June 2018.

[13] Kota, S., Flick, P., and Collier, F., "Flight Testing of the FlexFloil™ Adaptive Compliant Trailing Edge," AIAA Paper 2016-0036, January 2016.

[14] Miller, E. J., Cruz, J., Lung, S.-F., Kota, S., Ervin, G., and Lu, K.-J., "Evaluation of the Hinge Moment and Normal Force Aerodynamic Loads from a Seamless Adaptive Compliant Trailing Edge Flap in Flight," AIAA Paper 2016-0038, January 2016.

[15] Herrera, C., Y., Spivey, N. D., and Lung, S.-F., "Aeroelastic Response of the Adaptive Compliant Trailing Edge Transition Section," AIAA Paper 2016-0467, January 2016.

[16] Federal Aviation Administration, "Noise Standards: Aircraft Type and Airworthiness Certification," Advisory Circular No.36-4C, July 15, 2003.
[17] Lockard, D. P. and Bestul, K. A., "The Impact of Local Meteorological Conditions on Airframe Noise Flight Test Data," Paper to be presented at the AIAA/CEAS Aeroacoustics Conference in Atlanta, Georgia, June 2018.
[18] Humphreys, W. M., Lockard, D. P., Khorrami, M. R., and McSwain, R., "Evaluation of Methods for In-Situ Calibration of Field-Deployable Microphone Phased Arrays," AIAA Paper 2017-4176, June 2017.
[19] AVEC Time Domain Beamforming Software, Ver. 2.70, AVEC, Inc., Blacksburg, VA, URL: http://www.avec-engineering.com/products.html, cited May 13, 2018.
[20] Bass, H. E., Sutherland, L. C., Zuckerwar, A. J., Blackstock, and D. T., Hester, D. M., "Atmospheric absorption of sound: Further developments," *Journal of the Acoustical Society of America*, 97(1), January 1995, pp. 680-683.